



HAL
open science

Solvent-free allylic oxidation of alkenes with O-2 mediated by Fe- and Cr-MIL-101

I. Y. Skobelev, A. B. Sorokin, K. A. Kovalenko, V. P. Fedin, O. A. Kholdeeva

► **To cite this version:**

I. Y. Skobelev, A. B. Sorokin, K. A. Kovalenko, V. P. Fedin, O. A. Kholdeeva. Solvent-free allylic oxidation of alkenes with O-2 mediated by Fe- and Cr-MIL-101. *Journal of Catalysis*, 2013, 298, pp.61-69. 10.1016/j.jcat.2012.11.003 . hal-00826358

HAL Id: hal-00826358

<https://hal.science/hal-00826358>

Submitted on 30 Sep 2022

HAL is a multi-disciplinary open access archive for the deposit and dissemination of scientific research documents, whether they are published or not. The documents may come from teaching and research institutions in France or abroad, or from public or private research centers.

L'archive ouverte pluridisciplinaire **HAL**, est destinée au dépôt et à la diffusion de documents scientifiques de niveau recherche, publiés ou non, émanant des établissements d'enseignement et de recherche français ou étrangers, des laboratoires publics ou privés.



Distributed under a Creative Commons Attribution - NonCommercial 4.0 International License

Solvent-free allylic oxidation of alkenes with O₂ mediated by Fe- and Cr-MIL-101

Igor Y. Skobelev^{a,b}, Alexander B. Sorokin^b, Konstantin A. Kovalenko^c, Vladimir P. Fedin^c, Oxana A. Kholdeeva^{a,*}

^a Borekov Institute of Catalysis, pr. Lavrentieva 5, Novosibirsk 630090, Russia

^b IRCÉLYON, CNRS, 2, Avenue A. Einstein, 69626 Villeurbanne Cedex, France

^c Nikolaev Institute of Inorganic Chemistry, pr. Lavrentieva 3, Novosibirsk 630090, Russia

Catalytic properties of Fe-MIL-101 and Cr-MIL-101 metal-organic frameworks in the solvent-free oxidation of cyclohexene and α -pinene with molecular oxygen have been explored. Both catalysts allow alkene oxidation under mild conditions (1 bar O₂, 40–60 °C) and afford allylic oxidation products. The nature of catalysis and the product distribution strongly depend on the nature of the transition metal. Cr-MIL-101 behaves as truly heterogeneous catalyst to give predominantly α,β -unsaturated ketones. Catalysis over Fe-MIL-101 has true heterogeneous nature only at 40 °C, producing mainly 2-cyclohexene-1-ol. At 50–60 °C, iron leaching into solution occurs, leading to cyclohexenyl hydroperoxide as the major product. Under optimal conditions, both catalysts can be reused several times without suffering a loss of the catalytic properties. Rate-retarding and rate-accelerating effects of inhibitors and initiators, respectively, indicate radical chain mechanism. Different pathways for transformation of hydroperoxide have been suggested to rationalize the observed differences in the reaction selectivities over Cr- and Fe-MIL-101.

1. Introduction

The allylic oxidation of olefins is an important synthetic process since the oxidation products, α,β -unsaturated ketones and alcohols, are valuable intermediates for the fine chemical industry [1–3]. Usually, homogeneous catalytic systems or stoichiometric processes based on such oxidants as manganese dioxide, selenium dioxide, or chromium trioxide are employed to accomplish allylic oxidations [2–5]. However, the use of the hazardous oxidants and difficulties related to separation and recycling of homogeneous catalysts make such synthetic procedures environmentally unfriendly and cost consumable. The development of catalytic systems based on clean oxidants and easily recyclable heterogeneous catalysts is, therefore, a challenging goal [2].

Chromium catalysts are well known for the selective oxidation of cyclic alkenes to α,β -unsaturated ketones using *tert*-butyl hydroperoxide (TBHP) as oxidant [2–4]. Cr(III)-containing pillared clays [6], aluminophosphates [7], and mesoporous silicates CrMCM-41 and CrMCM-48 [8,9] were reported to catalyze this reaction. However, hot catalyst filtration tests [10] revealed that in most cases, the observed catalysis was due to chromium species leached from the solid catalyst into solution during the oxidation process, and hence, had homogeneous nature.

Metal-organic frameworks (MOFs) have attracted considerable attention due to a unique combination of properties, such as extremely high surface areas, crystalline open structures, tunable pore size, and functionality. These features allow considering them as prospective materials for gas storage, molecular recognition, separation, and catalysis [11–19]. From a catalytic point of view, these materials are very attractive for applications in liquid-phase processes since they potentially combine advantages of both homogeneous and heterogeneous catalysts. Normally, MOFs are composed of spatially isolated metal atoms or clusters linked by polydentate organic ligands, resulting in a rigid porous network. An important feature of MOFs is a high content of uniform active metal sites regularly distributed over the material. These sites are readily accessible for reagents due to the rather large size of pore entrances. Until recently, low thermal, chemical, and solvolytic stabilities (relative to completely inorganic zeolites) limited the interest to the application of MOFs in catalysis. However, in 2005, Férey and co-workers reported the discovery of the mesoporous chromium terephthalate Cr-MIL-101, which showed a good resistance to air, water, common solvents, and thermal treatment up to 300 °C [20]. In 2009, Taylor-Pashow and co-workers published the synthesis of the iron-containing analog, Fe-MIL-101 [21]. The MIL-101 materials have a zeolite-type crystal structure comprising two kinds of cages with free internal diameters of 29 and 34 Å, accessible through microporous windows of ca. 12 and 16 Å. They have extremely large surface areas and numerous transition metal sites, which can be activated by heating in vacuum [22].

* Corresponding author. Fax: +7 383 330 95 73.

E-mail address: khold@catalysis.nsk.su (O.A. Kholdeeva).

Activated Cr-MIL-101 was found to catalyze cyanosilylation of benzaldehyde [23], sulfoxidation of thioethers with H₂O₂ [22], benzylic oxidation of tetralin [24], allylic oxidation of alkenes with TBHP [25], and oxidation of cyclohexane with O₂ and/or TBHP [26]. The allylic oxidation of alkenes was also possible using aqueous hydrogen peroxide as oxidant after modification of MIL-101 with active polyoxometalate complexes [27]. However, the MIL-101-based catalytic systems reported so far for the allylic oxidation required the use of toxic and/or flammable organic solvents such as benzene, chlorobenzene [25], or acetonitrile [27] and a hydroperoxide oxidant (H₂O₂ or TBHP). At the same time, solvent-free oxidations that employ molecular oxygen are significantly more attractive from both economic and environmental viewpoints. One of the main technological advantages of solvent-free processes is a possibility to obtain high concentrations of products in the final mixture (high volume yield) even at rather low substrate conversions.

In the present work, we explore the potential of both Cr- and Fe-MIL-101 as heterogeneous catalysts for the solvent-free allylic oxidation of two representative alkenes, cyclohexene (CyH) and α -pinene, with molecular oxygen under mild reaction conditions (1 bar O₂, 40–60 °C). A particular attention is given to investigation into the nature of catalysis and evaluation of the catalysts stability and reusability. An attempt of rationalizing the differences in the product selectivities achieved over Cr-MIL-101 and Fe-MIL-101 under various reaction conditions is made, considering oxidation mechanisms that could be involved.

2. Experimental

2.1. Materials

CyH and α -pinene were purchased from Sigma-Aldrich or Alfa-Aesar and purified prior to use by passing through a column filled with neutral alumina to remove traces of possible oxidation products, in particular, hydroperoxides. All other reactants were obtained commercially and used without further purification. Aqueous solution of TBHP (70%) was used as initiator.

2.2. Preparation and characterization of catalysts

Cr-MIL-101 was prepared following a procedure similar to that described by Férey et al. [20]. In a typical synthesis, a mixture of 1.2 g (3 mmol) of Cr(NO₃)₃·9H₂O, 500 mg of terephthalic acid (H₂bdc, 3 mmol), and 0.6 mL of 5 M HF (3 mmol) in 15 mL H₂O was heated at 220 °C for 8 h in a Teflon-lined stainless steel bomb. The resulting green solid was passed through a coarse glass filter to remove unreacted H₂bdc and then filtered through a dense paper filter. The green raw product was washed in hot dimethylformamide (DMF) (100 °C, 8 h, 2 times) and then in boiling ethanol (80 °C, 8 h, 2 times), filtered off, and dried overnight in an oven at 75 °C.

Fe-MIL-101 was prepared as described by Taylor-Pashow et al. [21] with some modifications. In a typical synthesis, a mixture of 0.675 g (2.45 mmol) of FeCl₃·6H₂O, 206 mg of H₂bdc (1.24 mmol), and 15 mL DMF was heated at 110 °C for 20 h in a Teflon-lined stainless steel bomb. The resulting brown solid was filtered off, and the raw product was purified by washing in hot ethanol (60 °C, 3 h, 2 times), filtered off, and dried in an oven (70 °C, 30 min).

The resulting MIL-101 materials were characterized with X-ray diffraction (XRD) and N₂ adsorption measurements. XRD patterns of the MIL-101 materials were in accordance with the literature [20,21]. The BET (Brunauer–Emmett–Teller) specific surface areas were in the range of 3200–3400 m² g⁻¹. Both catalysts were activated in vacuum at 100 or 150 °C (Cr-MIL-101) or at 70 °C (Fe-MIL-101) for 6 h prior to catalytic studies.

2.3. Catalytic runs and product analysis

Catalytic experiments were carried out in thermostated glass vessels connected with an oxygen balloon (1 bar O₂). The oxidation reactions were performed at 40–60 °C under vigorous stirring (500 rpm). Typically, the reactions were initiated by the addition of a small amount of TBHP (2–3 × 10⁻² mmol) to a mixture containing an organic substrate (1 mL of cyclohexene or 1.5 mL of α -pinene) and 13–26 mg of the catalyst preliminary activated in vacuum (see above). The reaction time was 16 h. Concentration of cyclohexenyl hydroperoxide (CyH-OOH) was determined by iodometric titration in 80% acetic acid in the presence of H₃PO₄ (the latter was added as a 10% v/v aqueous solution). Other reaction products were identified by gas chromatography–mass spectrometry (GC–MS) and quantified by GC techniques. Aliquots of the reaction mixture (25 μ L) were withdrawn periodically during the reaction course by a syringe through a septum. Each aliquot was diluted with 0.4 mL of acetonitrile containing 60 mg of PPh₃ and internal standard (biphenyl). The treatment of the reaction mixture with PPh₃ is required to reduce CyH-OOH, otherwise it decomposes in the GC injector, affecting the ratio of 2-cyclohexene-1-ol (CyH-ol) and 2-cyclohexene-1-one (CyH-one) [28]. The true concentration of CyH-ol was calculated as a difference between the value obtained by GC and the concentration of CyH-OOH determined iodometrically (reduction in CyH-OOH with PPh₃ gives an additional amount of CyH-ol). Before recycling, catalysts were filtered off, washed two times with 15 mL of ethanol at 60 °C for 2 h, activated in vacuum, and then reused. Turnover frequency values (TOF) were determined from initial rates of CyH consumption. TOF was calculated on the basis of all metal ions of MIL-101 framework (23 wt.%) although the real number of the catalytically active sites could be smaller.

2.4. Adsorption measurements

The product adsorption on Fe-MIL-101 and Cr-MIL-101 was studied following the methodology reported elsewhere [29]. A sample of 28 mg of Fe-MIL-101 or Cr-MIL-101 activated in vacuum at 70 or 100 °C, respectively, was stirred with cyclohexane during 2 h. Then, MIL-101 material was filtered off using a syringe-driven filter. A solution of product (0.05 M of CyH-one, CyH-ol or α -pinene oxide in cyclohexane, 1.5 mL) was passed through the filter containing MIL-101 saturated with cyclohexane (it was taken instead of cyclohexene to avoid a possible product formation), collected, and passed again several times until the constant concentration of the product in the filtrate was reached. The product concentration in the filtrate was monitored by GC. One passage took 30 s. All operations were carried out at room temperature. The equilibrium constant was evaluated using Langmuir adsorption model

$$\theta = \frac{KC}{1 + KC} \quad (1)$$

and the mass balance equation

$$C_0V = CV + n\theta \quad (2)$$

where K is the adsorption constant, M⁻¹; V is the total volume of the product solution, L; C_0 is the initial product concentration, M; C is the equilibrium product concentration, M; n is the number of sorption sites (metal centers), mol; and θ is the degree of filling of the metal centers. Combining Eqs. (1) and (2), we can express the adsorption constant K by:

$$K = \frac{V(C_0 - C)}{C(n - V(C_0 - C))} \quad (3)$$

Eq. (3) was used for evaluation of the adsorption constants for CyH-ol, CyH-one and α -pinene oxide.

2.5. Instrumentation

GC analyses were performed using a gas chromatograph Agilent 4890D equipped with a flame ionization detector and a 30 m × 0.25 mm VF-5 MS capillary column or gas chromatograph Chromos GC-1000 equipped with a flame ionization detector and a 30 m × 0.25 mm BPX-5 capillary column. GC-MS analyses were carried out using a gas chromatograph HP 6890 (a 50 m × 0.25 mm DB-5 MS capillary column) equipped with a mass-selective detector Agilent MSD 5973. Fourier transform infrared spectroscopy (FT-IR) measurements were performed using KBr pellets containing 0.3 wt.% of sample on a Bruker Vector 22 or Bruker Vertex 80 spectrometer in the 400–4000 cm⁻¹ range. Nitrogen adsorption at 77 K was measured using an ASAP-2020 instrument (Micrometrics) or Sorbtometr M within the partial pressure range of 10⁻⁶–1.0. Elemental analysis was performed on HORIBA Jobin Yvon Activa ICP-OES (IRCELYON). For XRD measurements, Shimadzu XRD 7000S or DRON-3 M instruments were used.

3. Results and discussion

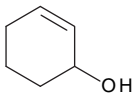
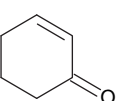
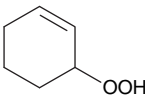
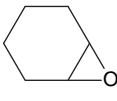
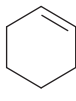
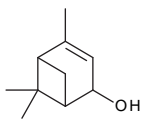
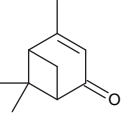
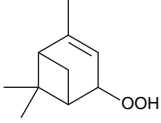
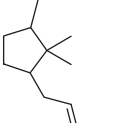
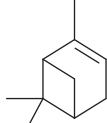
3.1. Product study

Both Fe-MIL-101 and Cr-MIL-101 mediated allylic oxidation of CyH and α -pinene with molecular oxygen under mild reaction conditions (1 atm O₂, 40–60 °C) without use of any organic solvent other than substrate. The oxidation reactions were initiated by addition of a small amount of TBHP (2–3 × 10⁻² mmol). The main results are presented in Table 1 along with the results of blank experiments. With CyH as substrate, both catalysts gave the unsaturated alcohol and ketone, CyH-ol and CyH-one, along with hydroperoxide CyH-OOH as major products. The formation of cyclohexene oxide was a minor reaction (less than 4%). Traces of

2,3-epoxy-cyclohexanone, 2,3-epoxy-cyclohexanol, bis-cyclohexenyl, and 1-chloro-2-cyclohexanol (the latter was found only in the presence of Fe-MIL-101) were identified by GC-MS technique. No derivatives of carboxylic acids were identified after methylation of the reaction mixture with trimethylsilyldiazomethane. A blank experiment showed that CyH oxidation does not occur in the absence of catalyst under the conditions employed (Table 1, run 1). On the other hand, only traces of the oxidation products (ca. 1% totally) were observed after 16 h when Fe-MIL-101 catalyst was used without TBHP initiator (Table 1, run 2). Hence, the blend of the catalyst and initiator is required to accomplish the oxidation reaction.

The product distribution and substrate conversion acquired over Fe-MIL-101 strongly depended on the reaction temperature. CyH-OOH predominated among the oxidation products at 50 and 60 °C, and the ratio of CyH-one and CyH-ol versus CyH-OOH augmented with increasing the reaction temperature. The total yield of the allylic oxidation products (CyH-OOH, CyH-one and CyH-ol) as well as the CyH-one/CyH-ol molar ratio also increased (Table 1, run 3 vs 4 and run 5 vs 6). However, the product distributions appeared to be quite similar for both temperatures while compared at close substrate conversions. Thus, selectivities to CyH-one, CyH-ol, and CyH-OOH were 22, 11, and 63%, respectively, at 27% conversion achieved at 50 °C (Table 1, run 3), while at 60 °C, they were 25, 10, and 60%, respectively, at 22% conversion (Fig. 1a). Interestingly, a similar product distribution was reported by Van Sickle et al. [30] for CyH autoxidation in the presence of conventional radical initiators: 80% CyH-OOH, 7% CyH-OH, 5% CyH-one, and 1% CyH oxide. This similarity strongly suggests that at 60 °C, over Fe-MIL-101 homogeneous cyclohexene autoxidation process contributes significantly to the product formation, and indeed, this was confirmed by hot filtration experiments (*vide infra*). The increase in metal to substrate molar ratio, [M]:[CyH], from 1:180 to 1:90 had a small (if any) effect on the substrate conversion and on the ratio be-

Table 1
Alkene oxidation with O₂ over Fe-MIL-101 and Cr-MIL-101^a.

Run	Catalyst	[M]:[CyH]	T, °C	Product selectivity, %					Substrate conversion, %
									
1	–	–	60	–	–	–	–	–	–
2	Fe-MIL-101 ^b	1:180	60	–	–	–	–	–	<1
3	Fe-MIL-101	1:180	50	11	22	63	4	–	27
4	Fe-MIL-101	1:180	60	14	36	46	4	–	44
5	Fe-MIL-101	1:90	50	6	31	59	4	–	32
6	Fe-MIL-101	1:90	60	7	43	46	4	–	44
7	Fe-MIL-101	1:180	40	58	15	27	–	–	8
8	Fe(acac) ₃ ^c	1:2 × 10 ⁵	60	9	23	59	9	–	44
9	Cr-MIL-101	1:180	50	25	58	17	–	–	12
10	Cr-MIL-101 ^d	1:180	50	20	60	20	–	–	10
11	Cr-MIL-101	1:90	60	38	56	6	–	–	16
									
12	–	–	60	1	1	2	–	–	4
13	Fe-MIL-101	1:180	40	33	–	25	33	9	12
14	Cr-MIL-101	1:90	60	31	39	14	8	8	26

^a Reaction conditions: 1 mL of alkene, 1 bar O₂, 13 or 26 mg of catalyst activated at 70 °C (Fe) or 100 °C (Cr), TBHP 0.02 mmol, 16 h.

^b No TBHP was added.

^c 5 ppm Fe.

^d Catalyst activation temperature 150 °C.

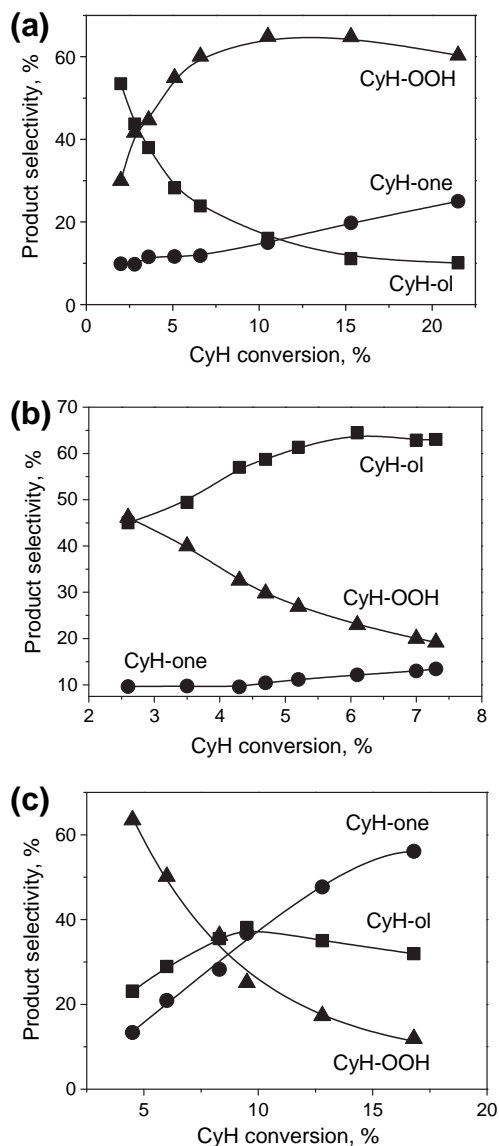


Fig. 1. Product selectivity versus substrate conversion for Fe-MIL-101 at 60 °C (a) and 40 °C (b) as well as Cr-MIL-101 at 60 °C (c).

tween the sum of CyH-one and CyH-ol and CyH-OOH. However, the relative amount of CyH-one with respect to CyH-ol was increased at higher catalyst loadings (Table 1, run 3 vs 5 and run 4 vs 6).

Interestingly, decreasing the reaction temperature from 50 to 40 °C resulted in a dramatic change in the product distribution (Table 1, run 7). Indeed, CyH conversion achieved only 8% after 16 h and CyH-ol became the main product formed with 58% selectivity, while selectivity to the other products was rather low (15% CyH-one and 27% CyH-OOH). Importantly, at 60 °C, Fe-MIL-101 provided 62% of CyH-OOH and only 20% of CyH-ol at the same substrate conversion (Fig. 1a). Therefore, the observed difference in the product distribution (Fig. 1a and b) cannot be associated with the effect of conversion. Most probably, different profiles of product distribution at 40 and 60 °C might be caused by changes in the rate-limiting step and/or entire reaction mechanism.

Cr-MIL-101 showed a lower CyH conversion under the same reaction conditions than Fe-MIL-101 (Table 1, run 3 vs 9 and run 6 vs 11). The selectivity toward CyH-one/-ol was much higher for Cr-MIL-101 at the same reaction temperature and conversion (compare Fig. 1a and c). Thus, the CyH-one/-ol selectivity attained 94% at 16% CyH conversion, while Fe-MIL-101 provided only 32%

CyH-one/-ol selectivity at the same conversion. The dependences of the product distribution on the CyH conversion at 60 °C differ significantly for Fe-MIL-101 (Fig. 1a) and Cr-MIL-101 (Fig. 1c), suggesting different reaction mechanisms. While for Fe-MIL-101, the selectivity to CyH-OOH strongly increased at the beginning of the reaction, the opposite trend was observed for Cr-MIL-101. The increase in the catalyst activation temperature led to minor changes in the product distribution and substrate conversion (Table 1, run 9 vs 10).

Oxidation of α -pinene (Table 1, runs 13 and 14) was studied under the conditions which allow true heterogeneous catalytic process (*vide infra*). The total alkene conversion achieved over both Cr- and Fe-MIL-101 was ca. 1.5 times higher than CyH conversion attained under the same conditions (Table 1, compare runs 7 and 13 or 11 and 14, respectively). Cr-MIL-101 afforded mostly verbenol (31%) and verbenone (39%) (Table 1, run 14) while Fe-MIL-101 favored the formation of verbenol (33%) and campholenic aldehyde (33%) (Table 1, run 13). With both catalysts, α -pinene oxide was the minor reaction product (8–9% selectivity). Only traces of verbenone were found for α -pinene oxidation over Fe-MIL-101. Thus, with both cyclohexene and α -pinene, only Cr-MIL-101 produces a significant amount of the corresponding unsaturated ketones.

Hermans et al. have demonstrated that α -pinene easily forms epoxide in autoxidation processes upon the addition of peroxy radicals to the C=C bond followed by a unimolecular rearrangement [31,32]. The low epoxide yields observed in the presence of Fe-MIL-101 and Cr-MIL-101 can be explained by several reasons. First, some amounts of the epoxide could be adsorbed by the catalyst. Indeed, the adsorption constant for α -pinene oxide on Fe-MIL-101 was evaluated to be ca. 30 M^{-1} (see Experimental for details). Consequently, under the concentration conditions of run 13 (Table 1), the maximum amount of α -pinene oxide adsorbed on Fe-MIL-101 could be estimated as $38 \mu\text{mol}$, while the amount of the epoxide in the solution is $150 \mu\text{mol}$. Note that the real amount of the adsorbed epoxide could be lower due to the concurrent adsorption of α -pinene and other oxidation products and higher reaction temperature. Second, α -pinene oxide could be transformed during the oxidation process into campholenic aldehyde and/or other products. To verify this assumption, we performed two additional experiments. In the first one, we added α -pinene oxide (0.03 M) to the reaction mixture containing α -pinene and catalyst before starting the reaction. No significant increase in the rate of campholenic aldehyde formation was observed during, at least, 5 h. In the second experiment, where 0.5 M of α -pinene oxide was added to an inert solvent, cyclohexane, containing the catalyst, we observed a pronounced decrease in α -pinene oxide concentration (ca. 40% conversion after 2 h at 40 °C), and GC-MS identified campholenic aldehyde as the main reaction product. Therefore, transformation of α -pinene oxide to the aldehyde cannot be ruled out. Finally, the catalyst could affect the peroxy over alkoxy radical concentration ratio. Indeed, the increase in the alkoxy radical concentration would favor allylic oxidation versus epoxidation which occurs via addition of peroxy radical to the alkene double bond. However, further studies are needed to verify this hypothesis.

3.2. Catalyst stability and recycling

Hot catalyst filtration tests [10] were performed to verify the nature of catalysis in the catalytic systems studied. The test carried out at 60 °C with Fe-MIL-101 revealed a significant contribution of homogeneous catalysis (Fig. 2a). Elemental analysis of the filtrate showed minor iron leaching (7 ppm). It is well known that transition metals are able to catalyze oxidation reactions, even when they are present in trace amounts [7,10]. Indeed, CyH oxidation performed in the presence of 5 ppm of $\text{Fe}(\text{acac})_3$ (Table 1, run 8) resulted in 44% CyH conversion. The product selectivities were close

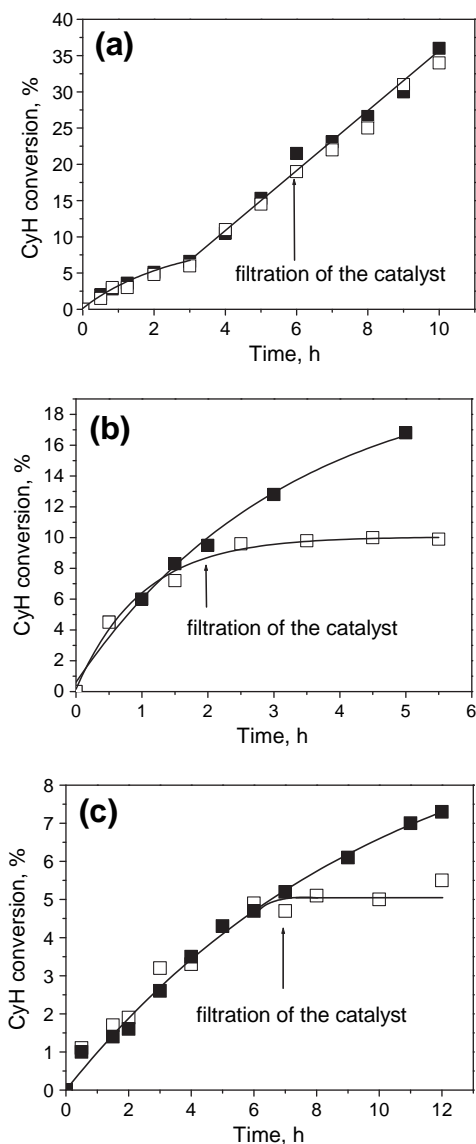


Fig. 2. Hot catalyst filtration test for Fe-MIL-101 (a) and Cr-MIL-101 (b) at 60 °C as well as Fe-MIL-101 at 40 °C (c).

to those observed for the Fe-MIL-101-catalyzed reaction at 60 °C (Table 1, run 4). Thus, we may conclude that catalysis observed with Fe-MIL-101 at 60 °C is due to active iron species leached into solution during the oxidation process. On the contrary, Cr-MIL-101 demonstrated much better stability than Fe-MIL-101 and behaved as truly heterogeneous catalyst at 60 °C, as proved by the hot filtration test (Fig. 2b). It should be noted that at a lower temperature (e.g., 40 °C), Fe-MIL-101 can also act as truly heterogeneous catalyst (Fig. 2c). According to the elemental analysis data, iron leaching in this case was below 1 ppm.

Finally, the recycling behavior of Fe-MIL-101 and Cr-MIL-101 was studied in CyH oxidation under the conditions where these catalysts certainly work as true heterogeneous ones. Both MIL-101 materials retained their catalytic properties during at least four consecutive runs (Table 2).

FT-IR spectroscopic studies revealed the presence of the characteristic bands of the MIL-101 metal-organic framework after four catalyst reuses (Fig. 3). The XRD measurements confirmed that Cr-MIL-101 preserved its structure after several reuses (Fig. 4a). However, a partial destruction of Fe-MIL-101 during the oxidation reaction occurred (Fig. 4b). The higher stability of Cr-MIL-101

Table 2
Recycling of Fe-MIL-101 and Cr-MIL-101 in CyH autoxidation.

Catalyst	Substrate conversion,%	Main product selectivity,%
Fe-MIL-101 ^a	9 (8, 9, 8) ^b	57 (55, 58, 56) ^{b,c}
Cr-MIL-101 ^d	16 (15, 17, 16) ^b	56 (58, 56, 57) ^{b,g}

^a 1 mL CyH, [Fe]:[CyH] = 1:180, 40 °C, 16 h.

^b In parentheses, 2nd, 3rd and 4th reuses.

^c CyH-ol selectivity.

^d 1 mL CyH, [Cr]:[CyH] = 1:90, 60 °C, 16 h.

^g CyH-one selectivity.

toward degradation during the catalytic process correlates with its higher thermal stability (300 °C [20] versus 150 °C for Fe-MIL-101 [33]). According to the N₂ adsorption data, the surface area decreased for both catalysts after their reuse. Thus, the surface area of Cr-MIL-101 diminished from 3400 to 1582 m²·g⁻¹, most probably, due to pore blockage by reaction products. In turn, the surface area of Fe-MIL-101 dropped from 3200 to 188 m²·g⁻¹ in accordance with the partial destruction of the MOF framework established by XRD (Fig. 4b).

3.3. Comparison with other catalytic systems

A comparison of the catalytic properties of Fe- and Cr-MIL-101 with some representative catalysts previously reported for CyH oxidation with molecular oxygen is given in Table 3. For all Cr-containing catalysts, including Cr-MIL-101, the main oxidation product was CyH-one, which indicates that the nature of active metal determines the oxidation mechanism. Chromium-containing molecular sieves allow achieving higher conversions of CyH than Cr-MIL-101 or Fe-MIL-101. Mesoporous Cr-MCM-41 showed the highest substrate conversion and enone selectivity but suffered from significant chromium leaching [34]. For Cr-APO5, the issue of metal leaching was not addressed, and the nature of catalysis remained unclear [34]. It is worth of noting that Cu-MOF [35] and Co-MOF [36] produced CyH-OOH as the main oxidation product. Co-MOF provided a high substrate conversion but in the presence of the organic solvent (0.6 M CyH in MeCN). The Fe/SiO₂ catalyst demonstrated a high CyH conversion at 78 °C in acetonitrile solution (1 M CyH) [37]. Unfortunately, the problem of the iron leaching was not addressed for this system, and no analysis for hydroperoxide formation was performed. Fe(BTC) metal-organic framework showed CyH conversion close to Fe-MIL-101 but at higher temperature and oxygen pressure [38]. Over both Fe(BTC) and Fe/SiO₂ catalysts, CyH-one predominated among the oxidation products. In contrast, Fe-MIL-101 afforded CyH-ol as the major product. This difference might be rationalized if we take into account more severe conditions applied for Fe(BTC) (100 °C, 5 bar O₂) or Fe/SiO₂ (78 °C, 1 bar O₂) compared to Fe-MIL-101 (40 °C and 1 bar O₂). Yet, different reaction mechanisms cannot be ruled out.

3.4. Mechanistic study

To assess the role of external diffusion in the oxidation process, we investigated the influence of the rate of stirring of the reaction mixture on the oxidation process. The increase in the rate from 500 to 1000 rpm did not affect the rate of CyH oxidation over Cr-MIL-101 at 60 °C (TOF 7 h⁻¹). In contrast, the reaction rate over Fe-MIL-101 at 40 °C increased significantly (TOF 7 versus 2 h⁻¹), indicating more efficient oxygen diffusion into the reaction mixture. Importantly, the product distribution remained unchanged. No further increase in TOF was observed upon increasing the stirring rate from 1000 to 1500 rpm.

The question of internal diffusion limitation is very important in the investigation into liquid-phase heterogeneous reactions over

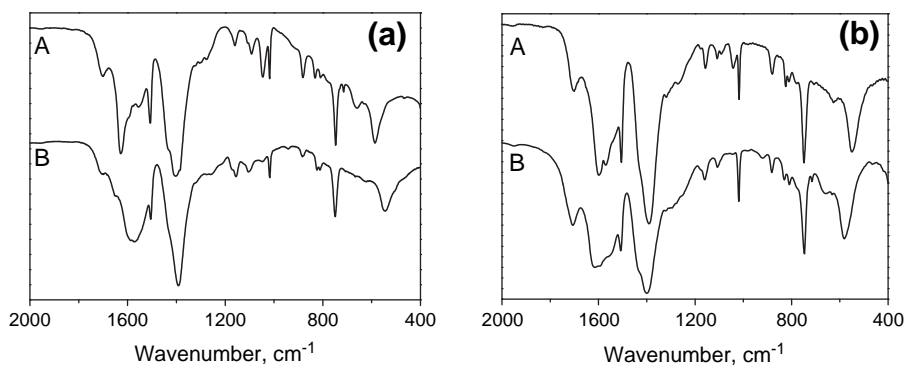


Fig. 3. FT-IR spectra of initial MIL-101 sample (curves A) and after 4 catalyst reuses (curves B) for Fe-MIL-101 (a) and Cr-MIL-101 (b).

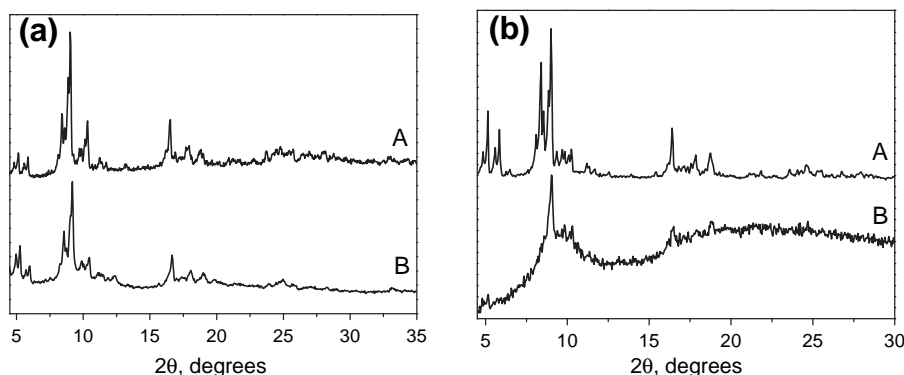
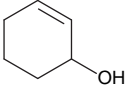
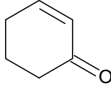
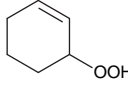

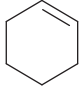


Fig. 4. XRD patterns of initial sample (curves A) and after 4 catalytic cycles (curves B) for Cr-MIL-101 (a) and Fe-MIL-101 (b).

Table 3
Catalytic performances of MIL-101 in solvent-free CyH oxidation with O₂ (1 bar) in comparison with other catalysts.

Catalyst	T, °C (time, h)	Product selectivity, %					Substrate conversion, %	Metal leaching	Ref.
									
Cr-MIL-101	60 (16)	38	56	6	–	16	<1 ppm	This work	
Fe-MIL-101	40 (16)	58	15	27	–	8	<1 ppm	This work	
Cr-MCM-41	70 (24)	11.2	71.2	14.2	3.4	52	56 ppm	[34]	
Cr-APO5	70 (24)	28	51	16	5	25	n.d. ^a	[34]	
Cu-MOF ^b	45 (15)	4	7	87	2	8	No leaching	[35]	
Co-MOF ^{c,d}	35 (24)	8	16	76	–	35	<1.1 ppm	[36]	
Fe ^{III} /SiO ₂ ^{d,e}	78 (10)	17	76	– ^h	5	98	n.d. ^a	[37]	
Fe-MOF ^{f,g}	100 (2)	38	59	–	3	12	No leaching	[38]	

^a Not determined.

^b [Co₄O(bdpb)₃], bdpb = 1,4-bis[(3,5-dimethyl)-pyrazol-4-yl]benzene.

^c Cu(bpy)₂(H₂O)₂(BF₄)₂, bpy = 4,4-bipyridine.

^d Acetonitrile was used as solvent.

^e Oxygen flow 20 mL/min.

^f Basolite F300 [Fe(BTC)] MOF, BTC = benzene-1,3,5-tricarboxylate.

^g 5 bar O₂.

^h No peroxide analysis was performed.

solid porous catalysts. Recently, it was found that oxidation of diphenylmethane (DPM) with TBHP catalyzed by Fe-MIL-100 revealed similar reaction rates regardless of the average particle size of the catalyst, while the activity of the Fe-MIL-100 samples in the oxidation of more bulky triphenylmethane (TPM) largely depended on this parameter, indicating that diffusion limitation within the MOF pores takes place for the bulky TPM substrate [39]. Molecules of CyH and its oxidation products are smaller than DPM molecule, while the cage entrances of MIL-101 (12 and 16 Å) are larger than

windows of MIL-100 (8.6 Å). Since no internal diffusion limitation was observed for the DPM oxidation over MIL-100, one can suggest that the same should be true in the case of CyH oxidation over MIL-101.

To verify this assumption, the adsorption kinetics of CyH-one and CyH-ol onto Cr- and Fe-MIL-101 was studied (see Experimental for details). The adsorption curves show that the adsorption equilibrium was reached after 1.5 and 1 min for Cr-MIL-101 and Fe-MIL-101, respectively (Fig. 5). Given in mind that the reaction

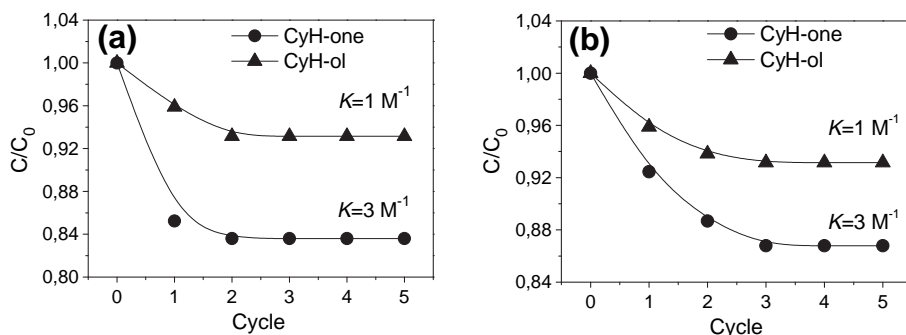


Fig. 5. Sorption of CyH-one and CyH-ol on Fe-MIL-101 (a) and Cr-MIL-101 (b) at room temperature. One cycle corresponds to 30 s.

time was typically 16 h, and the internal diffusion is hardly expected to be the rate-limiting step of the overall oxidation process. The values of the sorption equilibrium constants K estimated from eq. 3 are 1 and 3 M^{-1} for CyH-ol and CyH-one, respectively. Although these values were determined for room temperature and cannot be directly used for computation of the product sorption at the reaction temperatures, we may assume that adsorption of the oxidation products on the active metal sites could, in principle, hinder the reaction. To check this possibility, we added a solution of CyH-one and CyH-ol (ca. 0.5 M each, the concentration close to the value that was normally observed at the end of the reaction) into the reaction mixture at half of the maximal CyH conversion. The reaction stopped completely (Fig. 6). When only CyH-one (1.0 M) was added, the effect was similar. Hence, inhibition by the reaction products can be responsible for the termination of the CyH oxidation process after achieving a certain level of substrate conversion and product concentration. The situation changes dramatically when the active metal leaches into solution. Indeed, in the case of Fe-MIL-101 and the reaction temperature above 40°C , much higher CyH conversions could be achieved, and the product distribution changed drastically (Table 1).

As was mentioned before, the presence of both catalyst and initiator (TBHP) is necessary to accomplish alkene oxidation with molecular oxygen. In turn, the addition of a conventional inhibitor of radical chain processes (ionol) at half of the maximal CyH conversion immediately stopped the reaction over both Fe- and Cr-MIL-101 (Fig. 7). This could be, in principle, explained either by suppression of the growth of radical chains in autoxidation process or by adsorption of the inhibitor on the active metal sites, which may lead to the catalyst poisoning. Since the total amount of ionol introduced into the reaction mixture ($5 \mu\text{mol}$) was at least 10 times less than the

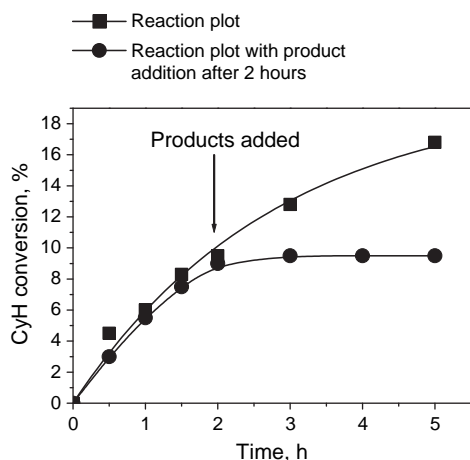
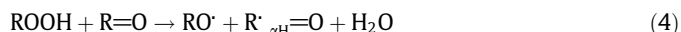


Fig. 6. Effect of the addition of CyH-one/CyH-ol mixture on the reaction over Cr-MIL-101.

total amount of the metal sites ($50\text{--}100 \mu\text{mol}$), catalyst poisoning by the inhibitor can hardly be expected. Hence, the reaction stopped, most likely, because of the interaction of the inhibitor with radicals responsible for the chain propagation. The observed effects of the initiator and inhibitor on the reaction rate point out radical chain nature of the CyH oxidation process over both MIL-101 catalysts. Since the control reaction without catalyst (but with TBHP initiator) exhibited a negligible conversion (Table 1, run 1), it is reasonable to suppose that thermal homolytic dissociation of hydroperoxide cannot be the principal initiation step and that MIL-101 participate, at least, in the chain initiation.

It is well known that the primary oxidation product in radical chain oxidation of hydrocarbons is a hydroperoxide, ROOH [40–42]. Further transformations of ROOH may include its homolytic decomposition over a catalyst (this process is responsible for the chain initiation/branching) and/or heterolytic decomposition leading to molecular products. The homolytic decomposition is described by the widely accepted Haber–Weiss mechanism that normally operates in the presence of transition metal ions [43,44], while the heterolytic decomposition may involve dehydration and/or disproportionation reactions.

In principle, unsaturated ketones can favor chain branching [45] through interaction with hydroperoxide ROOH:



If this occurred, one might expect that addition of CyH-one to the reaction mixture would increase the oxidation rate. However, an opposite effect (Fig. 6) was observed, and hence, we may exclude a significant contribution of reaction (4) to the overall oxidation process.

Since the product distribution in CyH and α -pinene oxidation differs markedly for Cr-MIL-10 and Fe-MIL-101, one can assume that further transformation of initially formed hydroperoxides proceeds via different pathways over these catalysts. Based on the literature [2,40–42,44] and the results obtained in this work, we can envisage a tentative mechanism for CyH oxidation over the MIL-101 catalysts as a sequence of steps shown in Scheme 1.

Indeed, Cr-containing catalysts are known to produce a high yield of cyclohexanone in the oxidation of cyclohexane due to their ability to favor dehydration of cyclohexyl hydroperoxide [46,47] and oxidation of alcohol to ketone [48,49]. Sheldon and co-workers studied CyH-OOH decomposition over chromium-containing porous solids, CrAPO-5 and CrS-1, and soluble complex $\text{Cr}(\text{acac})_3$ and found that all of them produced ca. 70% of CyH-one and 30% of CyH-ol [50], which is close to the results that we acquired in CyH oxidation using Cr-MIL-101. Consequently, the product distribution obtained over Cr-MIL-101 is likely due to CyH-OOH heterolytic decomposition and/or dehydration on the chromium active sites. Additionally, we found that Cr-MIL-101 is able to catalyze the oxidation of CyH-ol to CyH-one with molecular oxygen, providing 18% alcohol conversion after 4 h at 60°C in cyclohexane solution.

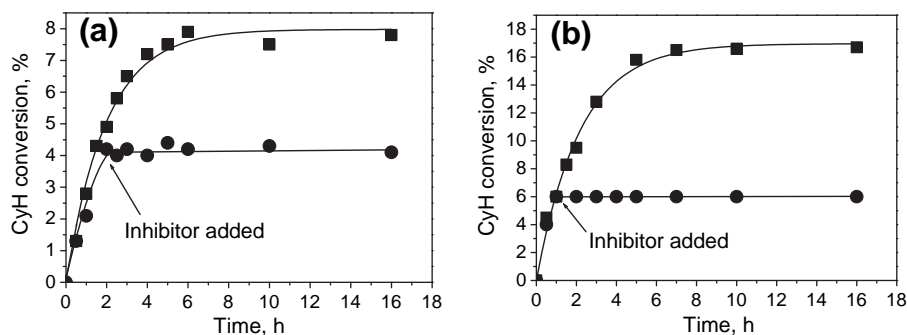
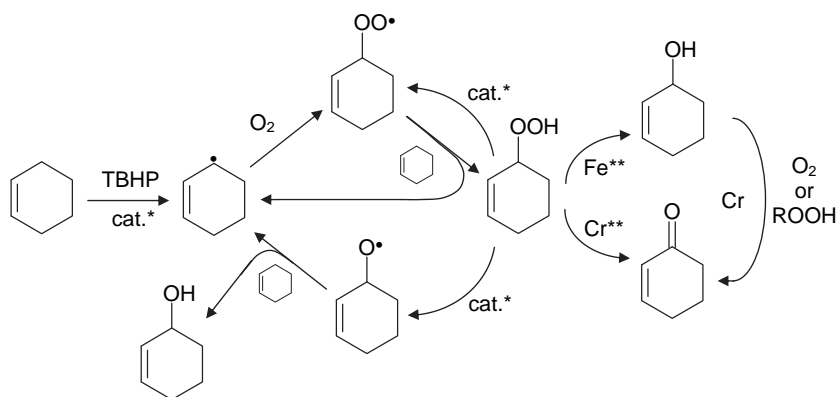


Fig. 7. Effect of inhibitor (ionol, 5 μmol) on the CyH oxidation rate over Fe-MIL-101 (a) and Cr-MIL-101 (b).



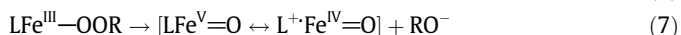
Scheme 1. Possible CyH oxidation pathways over MIL-101 catalysts: * radical chain pathway, ** non-radical chain pathway. Chain termination steps are not shown.

It is well known that conclusions about reaction mechanisms based on the product analysis solely should be drawn with precautions [51]. Nevertheless, the sharp difference in the product selectivity observed at 60 °C in the presence of homogeneous iron species and at 40 °C for the truly heterogeneous catalyst Fe-MIL-101 certainly indicates different oxidation pathways. In the former case, the product selectivity is classic for radical chain autoxidation [30,40–42]. At the same time, the product distribution observed for Fe-MIL-101 at 40 °C (58% of CyH-ol and just 15% of CyH-one) is quite unusual for radical-driven autoxidation processes where the alcohol to ketone (A/K) molar ratio normally does not exceed 2 [49,52–54]. Thus, the A/K molar ratio of ca. 1.4 (at least, at the beginning of the reaction) was found for cyclohexane autoxidation in the presence of Co(acac)₂ [49]. On the other hand, some examples of well-disguised radical reactions showing unusual selectivity, for example, the oxidation of alkanes with TBHP as oxidant catalyzed by Fe^{III}(TPA) (TPA = tris(2-pyridylmethyl)amine) complexes where alcohol formed as a major product, illustrate a complex nature of this chemistry [55,56]. Although we cannot rule out completely a contribution of the Haber–Weiss mechanism [43] to the overall alkene oxidation process over Fe-MIL-101, the unusually high A/K molar ratio (ca. 3.9) encouraged us to assume the existence of an alternative pathway.

Once formed, ROOH may react with active metal sites to form an alkylhydroperoxo complex:

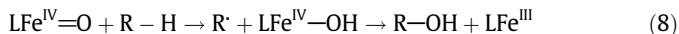


This complex can undergo either homolytic or heterolytic cleavage of the O—O bond to form LFe^{IV}=O or formally LFe^V=O adapting L⁺Fe^{IV}=O state according to reactions (6) and (7), respectively:



The mechanism of the O—O bond cleavage strongly depends on the nature of the hydroperoxide and ligand environment L. Heterolytic pathway frequently occurs in biological and bio-inspired systems when porphyrin-like macrocyclic ligand stabilizes the high oxidation state via participation of the ligand in the charge delocalization [57]. The LFe^V=O or L⁺Fe^{IV}=O species are known to be strong epoxidizing agents [58–60]. However, the amount of epoxide was low in the oxidation of CyH over Fe-MIL-101, especially, at 40 °C. Therefore, the formation of Fe^V=O seems unlikely, while the formation of LFe^{IV}=O and RO• via homolytic cleavage of O—O bond is in agreement with free radical oxidation mechanism deduced from the experimental observations. As was discussed above, radicals RO• abstract hydrogen atom from the allylic position of alkene, thus favoring allylic oxidation. In general, LFe^{IV}=O species show sluggish oxidizing properties. However, the increase in the oxidizing ability was previously observed for binuclear iron structures due to the presence of second metal ion in the active site [57]. A similar effect might be expected for Fe^{IV}=O species generated within tri-nuclear iron clusters which constitute the MIL-101 framework.

We suppose that the following reaction sequence may lead to the predominant formation of the enol product in the case of the heterogeneous alkene oxidation over Fe-MIL-101 at 40 °C:



Radical R• formed in reaction (8) could either interact with O₂ to form RO₂ radical and initiate a new chain or react with the LFe^{IV}—OH species to give an alcohol product via rebound reaction. When the oxidation process takes place within the MIL-101 cages, where high concentration of the iron centers is available, the interaction of R• with Fe^{IV}—OH may predominate. The situation changes dramatically when the active metal leaches from the Fe-MIL-101 matrix to the solution. The reaction of radical R• with O₂ to produce ROO• followed by H atom abstraction from alkene and formation of

ROOH becomes the main pathway because the concentration of iron species in solution is very low (<7 ppm), while the concentration of dioxygen is about 0.01 M [61]. Indeed, the ROOH product predominates at high temperature when Fe-MIL-101 is destroyed, and catalysis becomes homogeneous. However, further mechanistic studies are needed to verify the possibility of the formation of the iron-oxo species in the Fe-MIL-101 framework.

4. Conclusions

This study demonstrates that Fe and Cr-containing metal-organic frameworks of the MIL-101 family catalyze efficiently oxidation of alkenes with molecular oxygen under mild solvent-free conditions. By varying the nature of transition metal in the MIL-101 framework, it is possible to govern the oxidation selectivity. Cr-MIL-101 favors the formation of α,β -unsaturated ketones, while Fe-MIL-101 can produce higher amounts of allylic alcohols. The nature of catalysis over Cr-MIL-101 was proved to be true heterogeneous under all range of the conditions studied. In contrast, Fe-MIL-101 revealed a lower stability under turnover conditions and behaved as true heterogeneous only at 40 °C. The XRD and N₂ adsorption measurements clearly showed that the structure of Fe-MIL-101 partially collapsed after several reuses although FT-IR spectroscopy revealed the presence of the main characteristic bands of the MOF. Meanwhile, under optimal conditions both Cr- and Fe-catalysts could be recycled at least four times without loss of the catalytic properties. Since the reaction products inhibit the oxidation process through adsorption on the MOF active centers, the feasible alkene conversions are not high for one catalytic run. However, the employment of solvent-free conditions ensures high volume yield of the oxidation products even at rather low conversions. At the temperature higher than 40 °C, Fe-MIL-101 starts suffering from iron leaching, and catalysis becomes homogeneous, which results in much higher substrate conversion and change of the product selectivity (hydroperoxide turns out to be the main oxidation product).

With both Fe- and Cr-catalysts, the oxidation of alkenes proceeds through radical chain mechanism, as pointed out by the rate-retarding effect of the inhibitor (ionol) and rate-accelerating effect of the initiator (TBHP); however, different pathways (both radical chain and non-radical chain) may contribute to the product formation, resulting in different reaction selectivities. The metal-centered oxidation steps leading to unsaturated alcohol product are probably involved in the case of Fe-MIL-101, while dehydration of hydroperoxide and/or oxidation of alcohol to ketone over Cr-MIL-101 are responsible for the predominate formation of unsaturated ketones.

Acknowledgments

Dr. M.S. Melgunov is gratefully acknowledged for some N₂ adsorption measurements. The research was partially supported by the Russian Foundation for Basic Research (Grant 09-03-93109). I.Y.S. acknowledges French Embassy in Moscow for the doctoral fellowship. Work at the Nikolaev Institute of Inorganic Chemistry was supported by the State Contracts (1729.2012.3 and 02.740.11.0628).

References

[1] M. Hudlicky, *Oxidations in Organic Chemistry*, ACS Monograph Series, American Chemical Society, Washington, DC, 1990. p. 84.
 [2] R.A. Sheldon, in: R.A. Sheldon, H. van Bekkum (Eds.), *Fine Chemicals through Heterogeneous Catalysis*, Wiley-VCH, Weinheim, 2001, p. 519.

[3] E.F. Murphy, T. Mallat, A. Baiker, *Catal. Today* 57 (2000) 115.
 [4] J. Muzart, *Chem. Rev.* 92 (1992) 113.
 [5] N. Chidambaram, S. Chandrasekaran, *J. Org. Chem.* 52 (1987) 5048.
 [6] B.M. Choudary, A.D. Prasad, V. Swapna, V.L.K. Valli, V. Bhumra, *Tetrahedron* 48 (1992) 953.
 [7] H.E.B. Lempers, R.A. Sheldon, *Appl. Catal. A* 143 (1996) 137.
 [8] A. Sakthivel, S.E. Dapurkar, P. Selvam, *Appl. Catal. A* 246 (2003) 283.
 [9] S.E. Dapurkar, A. Sakthivel, P. Selvam, *New J. Chem.* 27 (2003) 1184.
 [10] R.A. Sheldon, M. Wallau, I.W.C.E. Arends, U. Schuchardt, *Acc. Chem. Res.* 31 (1998) 485.
 [11] J.L.C. Rowsell, O.M. Yaghi, *Micropor. Mesopor. Mater.* 73 (2004) 3.
 [12] A.K. Cheetham, C.N.R. Rao, R.K. Feller, *Chem. Commun.* (2006) 4780.
 [13] G. Férey, *Chem. Soc. Rev.* 37 (2008) 191.
 [14] A.U. Czaja, N. Trukhan, U. Muller, *Chem. Soc. Rev.* 38 (2009) 1284.
 [15] D. Farrusseng, S. Aguado, C. Pinel, *Angew. Chem. Int. Ed.* 48 (2009) 7502.
 [16] A. Corma, H. García, F.X. Llabrés i Xamena, *Chem. Rev.* 110 (2010) 4606.
 [17] M. Yoon, R. Srirambalaji, K. Kim, *Chem. Rev.* 112 (2011) 1196.
 [18] A. Dhakshinamoorthy, M. Alvaro, H. García, *Catal. Sci. Technol.* 1 (2011) 856.
 [19] Thematic issue on metal-organic frameworks, *Chem. Rev.* 112 (2012) 673.
 [20] G. Férey, C. Mellot-Draznieks, C. Serre, F. Millange, J. Dutour, S. Surblé, I. Margiolaki, *Science* 309 (2005) 2040.
 [21] K.M.L. Taylor-Pashow, J. Della Rocca, Z. Xie, S. Tran, W. Lin, *J. Am. Chem. Soc.* 131 (2009) 14261.
 [22] Y.K. Hwang, D.-Y. Hong, J.-S. Chang, H. Seo, M. Yoon, J. Kim, S.H. Jung, C. Serre, G. Férey, *Appl. Catal. A* 358 (2009) 249.
 [23] A. Henschel, K. Gedrich, R. Kraehnert, S. Kaskel, *Chem. Commun.* (2008) 4192.
 [24] J. Kim, S. Bhattacharjee, K.-E. Jeong, S.-Y. Jeong, W.-S. Ahn, *Chem. Commun.* (2009) 3904.
 [25] N.V. Maksimchuk, K.A. Kovalenko, V.P. Fedin, O.A. Kholdeeva, *Adv. Synth. Catal.* 352 (2010) 2943.
 [26] N.V. Maksimchuk, K.A. Kovalenko, V.P. Fedin, O.A. Kholdeeva, *Chem. Commun.* 48 (2012) 6812.
 [27] N.V. Maksimchuk, M.N. Timofeeva, M.S. Melgunov, A.N. Shmakov, Yu.A. Chesalov, D.N. Dymbtsev, V.P. Fedin, O.A. Kholdeeva, *J. Catal.* 257 (2008) 315.
 [28] G.B. Shul'pin, *J. Mol. Catal. A: Chem.* 189 (2002) 39.
 [29] H.L. Wang, J.L. Duda, C.J. Radke, *J. Colloid Interface Sci.* 66 (1978) 153.
 [30] D.E. Van Sickle, F.R. Mayo, R.M. Arluck, *J. Am. Chem. Soc.* 87 (1965) 4832.
 [31] U. Neuenschwander, F. Guignard, I. Hermans, *ChemSusChem* 3 (2010) 75.
 [32] U. Neuenschwander, I. Hermans, *Phys. Chem. Chem. Phys.* 12 (2010) 10542.
 [33] S. Bauer, C. Serre, T. Devic, P. Horcajada, J. Marrot, G. Férey, N. Stock, *Inorg. Chem.* 47 (2008) 7568.
 [34] S.E. Dapurkar, H. Kawanami, K. Komura, T. Yokoyama, Y. Ikushima, *Appl. Catal. A* 346 (2008) 112.
 [35] D. Jiang, T. Mallat, D.M. Meier, A. Urakawa, A. Baiker, *J. Catal.* 270 (2010) 26.
 [36] M. Tonigold, Y. Lu, A. Mavrandonakis, A. Puls, R. Staudt, J. Möllmer, J. Sauer, D. Volkmer, *Chem. Eur. J.* 17 (2011) 8671.
 [37] J. Mao, X. Hu, H. Li, Y. Sun, C. Wang, Z. Chen, *Green Chem.* 10 (2008) 827.
 [38] A. Dhakshinamoorthy, M. Alvaro, H. García, *J. Catal.* 289 (2012) 259.
 [39] A. Dhakshinamoorthy, M. Alvaro, Y.K. Hwang, Y.-K. Seo, A. Corma, H. García, *Dalton Trans.* 40 (2011) 10719.
 [40] E.T. Denisov, N.I. Mitskevich, V.E. Agabekov, *Liquid-Phase Oxidation of Oxygen-Containing Compounds*, Consultants Press, New York, 1977.
 [41] R.A. Sheldon, J.K. Kochi, *Metal-Catalyzed Oxidations of Organic Compounds*, Academic Press, New York, 1981.
 [42] E.T. Denisov, I.B. Afanas'ev, *Oxidation and Antioxidants in Organic Chemistry and Biology*, Taylor & Francis, Boca Raton, 2005.
 [43] F. Haber, *J. Weiss, Proc. R. Soc. London, A* 147 (1934) 332.
 [44] H. Weiner, A. Trovarelli, R.G. Finke, *J. Mol. Catal. A: Chem.* 191 (2003) 217.
 [45] U. Neuenschwander, I. Hermans, *J. Catal.* 287 (2012) 1.
 [46] J.D. Chen, J. Dakka, R.A. Sheldon, *Appl. Catal. A* 108 (1994) L1.
 [47] W. Buijs, R. Raja, J.M. Thoma, H. Wolters, *Catal. Lett.* 91 (2003) 253.
 [48] J.D. Chen, J. Dakka, E. Neeleman, R.A. Sheldon, *J. Chem. Soc., Chem. Commun.* (1993) 1379.
 [49] I. Hermans, J. Peeters, P.A. Jacobs, *Top. Catal.* 48 (2008) 41.
 [50] H.E.B. Lempers, J.D. Chen, R.A. Sheldon, *Stud. Surf. Sci. Catal.* 94 (1995) 705.
 [51] K.U. Ingold, P.A. MacFaul, in: B. Meunier (Ed.), *Biomimetic Oxidation Catalyzed by Transition Metal Complexes*, Imperial College Press, London, 2000, p. 45.
 [52] A. Ramanathan, M.S. Hamdy, R. Parton, T. Maschmeyer, J.C. Jansen, U. Hanefeld, *Appl. Catal. A* 355 (2009) 78.
 [53] A.P. Singh, N. Torita, S. Shylesh, N. Iwasa, M. Arai, *Catal. Lett.* 132 (2009) 492.
 [54] N. Turrà, A.B. Acuña, B. Schimmöller, B. Mayr-Schmölzer, P. Mania, I. Hermans, *Top. Catal.* 54 (2011) 737.
 [55] P.A. MacFaul, K.U. Ingold, D.D.M. Wayner, L. Que Jr., *J. Am. Chem. Soc.* 119 (1997) 10594.
 [56] J. Kim, R.G. Harrison, C. Kim, L. Que Jr., *J. Am. Chem. Soc.* 118 (1996) 4373.
 [57] A.B. Sorokin, E.V. Kudrik, *Catal. Today* 159 (2011) 37.
 [58] S. Tanase, E. Bouwman, *Adv. Inorg. Chem.* 58 (2006) 29.
 [59] P.D. Oldenburg, L. Que Jr., *Catal. Today* 117 (2006) 15.
 [60] O.Y. Lyakin, K.P. Bryliakov, G.J.P. Britovsek, E.P. Talsi, *J. Am. Chem. Soc.* 131 (2009) 10798.
 [61] R. Battino, T.R. Rettich, T. Tominaga, *J. Phys. Chem. Ref. Data* 12 (1983) 163.